

NUMERICAL SOLUTION OF MAGNETOHYDRODYNAMIC FLOW PROBLEM USING RADIAL BASIS FUNCTION BASED FINITE DIFFERENCE METHOD

M. P. JEYANTHI^{a,*}, S. GANESH^a, L. J. T. DOSS^b, A. PRABHU^b

^a*Sathyabama Institute of Science and Technology, Chennai 600119, India*

^b*Anna University, Chennai 600025, India*

This paper focuses on the application of Radial Basis Function generated Finite Difference Method (RBF-FD) to solve Magnetohydrodynamic (MHD) flow equation in a rectangular duct in the presence of the transverse external oblique magnetic field. Multiquadric (MQ) Radial Basis Function is used to obtain the numerical solution of the MHD flow problem. Accuracy of the solution can be improved by varying the shape parameter in MQ function. The solution obtained from RBF-FD method is compared with the analytical solution and classical Finite Difference solution. Contours are presented for various Hartmann numbers with different grid sizes and directions of the applied magnetic field. The behaviour of velocity and the magnetic field of the MHD flow have been studied using the contours.

(Received September 6, 2020; Accepted November 24, 2020)

Keywords: Magnetohydrodynamic flow, Radial basis function, Multi-quadric, Finite difference method, Radial basis function generated finite difference

1. Introduction

In this article, a numerical method based on Radial Basis Function generated Finite Difference method is presented for Magnetohydrodynamic (MHD) flow problem. In MHD flow, the fluid is electrically conducting unlike hydrodynamic flow. The electrostatic part of the electric field is due to the free and bound charges distributed in and around the fluid. The study of the flow of conducting fluids in ducts in the presence of transverse magnetic field is important, because of its practical applications like Magnetohydrodynamic (MHD) flow through channels in nuclear reactors, MHD flow meters, MHD generators, blood flow measurements, pumps, accelerators. One of the important problems in MHD flow is under the uniform magnetic field, the flow of incompressible viscous electrically conducting fluids in ducts. First, Hartmann and Lazarus [1] studied the MHD flow problem under the action of the transverse magnetic field.

Various forms of MHD problems with different combinations of conducting and non-conducting walls have been considered by several authors [2,3,4]. The analytical solution is available only for a few special cases. Thus, researchers are interested to apply numerical methods to get better solutions of MHD flows with different cross-sections such as square, rectangle, circle, ellipse, triangle etc., Tezer-Sezgin [5] used Differential Quadrature Method (DQM) to solve MHD flow in a rectangular duct. Using DQM, the problem can be solved for the range of Hartmann numbers 2 to 50. Various numerical methods like FDM [6,7], BEM [8] have been used for solving the MHD problem. DRBEM method used in [9] to solve the Laplace equation in different geometries of a duct, but solutions could not be obtained for Hartmann numbers more than 8. FDM was used in [10] to solve coupled non-dimensional equations with grid size 101×101 for Hartmann numbers less than 100 and for Hartmann number greater than 100 the mesh size was 201×201 . In most of the above-referenced papers, the solutions were given only up to $M = 250$. For Hartmann numbers, less than 10 the FEM solutions are presented in [11,12]. Further, for moderate Hartmann numbers (less than 100) Tezer Sezgin and Koksall [13] extended the solution. Then Demandy and Nagy [14] obtained the solution of MHD flow problem up to 1000. Later, the solution of MHD problem for the range of 10^2 to 10^6 is given by Nesliturk and Tezer-Sezgin [15].

* Corresponding author: prasannajeyanthim@gmail.com

In [16], the solution of the same problem using Boundary element method has been discussed for high Hartmann numbers till 10^5 .

Most of the numerical methods need structured meshes to solve a partial differential equation on any domain. In 1970 RBF methods were developed to overcome the structural requirements of existing numerical methods. Initially, RBFs were introduced to interpolate multidimensional scattered data. RBF methods were first studied by Ronald Hardy in 1968. Hardy [17] derived the two-dimensional Multiquadric (MQ) scheme to approximate geographical surfaces and magnetic anomalies. Hardy [18] developed one of the main RBF theory and application of MQ-biharmonic method. Kansa [19,20] showed that his modified MQ scheme is an excellent method not only for very accurate interpolation but also for partial derivative schemes. After Kansa's method, many papers were published for solving PDE. RBF based local method was introduced in [21] to solve Poisson equations. Wright and Fornberg [22] stated that of all the RBF methods tested, Hardy's Multiquadric method gave the most accurate results. The grid-free 'local' RBF-FD schemes have been developed to solve linear and non-linear, steady and unsteady convection-diffusion problems in [23]. Sanyasiraju and Chandhini [24] used the RBF method to solve unsteady incompressible viscous flows. The convergence behaviour of RBF-FD formula is discussed in [25]. The optimal shape parameter for MQ based RBF-FD at each node of the computational domain was presented in [26,27].

The RBF-FD method was used to solve diffusion and reaction-diffusion equations (PDEs) on closed surfaces [27], convective PDEs [28], in geosciences [29], Navier-Stokes equation [30] and heat transfer problem [31]. In all the above papers, the RBF-FD method has given a better solution which motivates to solve MHD flow problem using RBF-FD. The computational solution of the same problem using RBF-FD method up to Hartmann Number 90 has been discussed in [32]. The Radial Basis Function solution of problems defined in [33,34] are presented in [35].

In this paper, RBF-FD method is used to obtain the solution for MHD flow problem in a rectangular duct with insulated walls. First, the coupled equations are decoupled using a change of variables. Then each equation is solved using RBF-FD to obtain velocity and induced magnetic field. In this method, the Hartmann number can be increased from 1 to 1000 without any complications.

2. Radial basis function

The radial basis functions are initially considered as one of the powerful primary tools for interpolating multidimensional scattered data. Some of the applications of RBFs are in Cartography, neural networks, medical imaging, numerical solution of PDEs, learning theory and geographical research. The radial basis function is radially symmetric with respect to the center. The RBF-FD formulas are derived from RBF interpolants.

2.1. RBF interpolation

Let $u: \mathbb{R}^n \rightarrow \mathbb{R}$ be a sufficiently smooth function. Further, let $\bar{x}_j, j = 1, 2, \dots, n$ be a given set of nodal points in the domain of u , with $u_j, j = 1, 2, \dots, n$ being the known values of the function u at \bar{x}_j 's respectively. Let \bar{x} be the free variable point in the domain of u , at which an approximation for $u(\bar{x})$ through Radial Basis Function(RBF) is defined as follows, The RBF interpolation $s(\bar{x})$ of $u(\bar{x})$ is defined as the linear combination of radially symmetric functions that coincide $u(\bar{x})$ at $\bar{x}_j, j = 1, 2, \dots, n$ and is given by

$$u(\bar{x}) \approx s(\bar{x}) = \sum_{j=1}^n \lambda_j \phi(\|x - x_j\|) \quad (4)$$

where, $\| \cdot \|$ indicates Euclidean norm. The λ_j 's, $j = 1, 2, \dots, n$ can be computed from $u(\bar{x}_j) = s(\bar{x}_j)$ $j = 1, 2, \dots, n$.

$$\begin{bmatrix} \phi_{11} & \phi_{12} & \cdots & \phi_{1n} \\ \phi_{21} & \phi_{22} & \cdots & \phi_{2n} \\ \vdots & & & \\ \phi_{n1} & \phi_{n2} & \cdots & \phi_{nm} \end{bmatrix} \begin{bmatrix} \lambda_1 \\ \lambda_2 \\ \vdots \\ \lambda_n \end{bmatrix} = \begin{bmatrix} u(\bar{x}_1) \\ u(\bar{x}_2) \\ \vdots \\ u(\bar{x}_n) \end{bmatrix} \quad (5)$$

where, $\phi_{ij} = \phi(\|\bar{x}_i - \bar{x}_j\|)$. The Lagrange form of RBF interpolant was presented in [36].

Classifications of RBFs are infinitely smooth and piecewise smooth radial basis functions. The former feature has a shape parameter ε , by varying which the radial function can be varied from sharp-peaked one to very flat one. Some of the commonly used radial basis functions are given in Table 1. The RBF may have the shape parameter ε , in that case $\phi(r)$ can be replaced by $\phi(r, \varepsilon)$.

Table 1 Examples of Radial basis function.

Name of the RBF	$\phi(r) \geq 0$	order of RBF
Infinitely smooth RBF		
Multiquadric (MQ)	$\sqrt{1 + (\varepsilon r)^2}$	$\left\lceil \frac{1}{2} \right\rceil$
Inverse Multiquadric(IMQ)	$\frac{1}{\sqrt{1 + (\varepsilon r)^2}}$	0
Inverse Quadric (IQ)	$\frac{1}{1 + (\varepsilon r)^2}$	0
Generalized MQ (GMQ)	$(1 + (\varepsilon r)^2)^\nu$	$\left\lceil \frac{\nu}{2} \right\rceil$
Gaussian(GA)	$e^{-(\varepsilon r)^2}$	0
Piecewise-smooth		
Polyharmonic Spline	$r^\nu, \nu > 0, \nu \notin 2N$	$\left\lceil \frac{\nu}{2} \right\rceil$
Thin Plate Spline	$r^{2k} \log r$	k + 1

2.2. RBF-FD formula for derivatives

Let L be a linear differential operator (like $\partial / \partial x$, etc). In order to approximate L at the interior node x_i , the neighbouring nodes of x_i , say n_i nodes x_1, x_2, \dots, x_{n_i} are considered. The following are the three general strategies [23] for choosing neighbouring nodes.

- Central (C): The nodes which lie equidistant from the centre x_i
- Upwind (U): The nodes which lie in the direction of flow
- Hybrid (CU): The nodes are selected as a combination of U and C

The approximation of $Lu(\bar{x}_i)$ is expressed as the linear combination of the values of the function u at the neighbourhood points of x_i .

$$Lu(\bar{x}_i) = \sum_{j=1}^{n_i} w_j^i u(\bar{x}_j) \quad (6)$$

The RBF interpolant (4) is applied in the equation (6) and the weights are expected to give exact result compared to polynomial interpolation. Using equations (5) and (6) the weights can be calculated as in [37]

$$\begin{bmatrix} \phi_{11} & \phi_{12} & \cdots & \phi_{1n} \\ \phi_{21} & \phi_{22} & \cdots & \phi_{2n} \\ \vdots & & & \\ \phi_{n1} & \phi_{n2} & \cdots & \phi_{nn} \end{bmatrix} \begin{bmatrix} w_1^i \\ w_2^i \\ \vdots \\ w_{n_i}^i \end{bmatrix} = \begin{bmatrix} \mathcal{L}\phi(\|x_i - x_1\|) \\ \mathcal{L}\phi(\|x_i - x_2\|) \\ \vdots \\ \mathcal{L}\phi(\|x_i - x_n\|) \end{bmatrix} \quad (7)$$

The above system of equations can be represented in matrix form

$$\Phi w = \mathcal{L}(B(\bar{x}_i)) \quad (8)$$

Equations (6) to (8) describe the local scheme to approximate $\mathcal{L}u(\bar{x}_i)$ at each distinct node \bar{x}_i .

Implementation of RBF-FD scheme is similar to the Finite Difference method for both linear and nonlinear equation and also for the coupled equation.

3. Application RBF-FD Scheme to the MHD flow problem

The governing equations of steady laminar flow of an incompressible, viscous, electrically conducting fluid in a rectangular duct subject to a constant uniform imposed magnetic field in the standard non-dimensional form is

$$\nabla^2 V + M_x \frac{\partial B}{\partial x} + M_y \frac{\partial B}{\partial y} = -1 \quad \text{in } \Omega \quad (9)$$

$$\nabla^2 B + M_x \frac{\partial V}{\partial x} + M_y \frac{\partial V}{\partial y} = 0 \quad \text{in } \Omega \quad (10)$$

with the boundary conditions

$$V = B = 0 \quad \text{on } \partial\Omega \quad (11)$$

where, $M_x = M \sin \alpha$, $M_y = M \cos \alpha$, $M = (M_x^2 + M_y^2)^{\frac{1}{2}}$, Ω represents the cross-section of the duct, $\partial \Omega$ represents the boundary of the duct which is assumed to be insulated. $V(x, y)$, $B(x, y)$ represents the velocity and induced magnetic field respectively, and M denotes the Hartmann number. Here it is assumed that the applied magnetic field is parallel to the x-axis. $V(x, y)$, $B(x, y)$ are in the z-direction, which is the axis of the duct, and the fluid is driven through the duct by means of a constant pressure gradient. The duct walls are $x = 0$, $x = 1$, $y = -1$ and $y = 1$. Equation (9) and (10) may be decoupled by using the change of variables as follows.

$$U_1 = V + B \quad U_2 = V - B \quad (12)$$

Then equation (9) and (10) are of the form

$$\nabla^2 U_1 + M_x \frac{\partial U_1}{\partial x} + M_y \frac{\partial U_1}{\partial y} = -1 \quad \text{in } \Omega \quad (13)$$

$$\nabla^2 U_2 + M_x \frac{\partial U_2}{\partial x} + M_y \frac{\partial U_2}{\partial y} = -1 \quad \text{in } \Omega \quad (14)$$

with the boundary conditions

$$U_1 = U_2 = 0 \quad \text{on } \partial\Omega \quad (15)$$

By applying RBF-FD method to equation (13) gives,

$$\sum_{j=1}^{n_i} C_{ij} U_{ij} + M_x \sum_{j=1}^{n_i} D_{ij} U_{ij} + M_y \sum_{j=1}^{n_i} E_{ij} U_{ij} = -1 \quad (16)$$

where n_i is the number of neighbourhood points, C_{ij} is the weights corresponding to ∇^2 , D_{ij} are the weights corresponding to $\frac{\partial}{\partial x}$ and E_{ij} are the weights corresponding to $\frac{\partial}{\partial y}$ for each nodal point $i = 1, 2, \dots, n$. It is obvious that the Dirichlet boundary conditions can be substituted in equation (16) and this leads to the following system of equations.

$$AU = b \quad (17)$$

where, U is an unknown vector which consists of U values at all interior points, b is a known vector and A is a coefficient matrix. U_1 values can be obtained by solving the above system of equations. To find values of U_2 replace $M_x = -M_x$ and $M_y = -M_y$ in equation (16). Then the velocity and the induced magnetic field can be obtained using equation (12).

The analytical solution of the equations (9) & (10) is available for the particular case $\alpha = \pi / 2$ in [2]. When $\alpha = \pi / 2$, $M_x = M \sin \alpha = M$, $M_y = M \cos \alpha = 0$, the governing equations (9) & (10) becomes,

$$\nabla^2 V + M \frac{\partial B}{\partial x} = -1 \quad \text{in } \Omega \quad (18)$$

$$\nabla^2 B + M \frac{\partial V}{\partial x} = 0 \quad \text{in } \Omega \quad (19)$$

with the boundary conditions $V = B = 0$ on $\partial\Omega$

Using the equation (12), equation (18) and (19) can be decoupled as follows

$$\nabla^2 U_1 + M \frac{\partial U_1}{\partial x} = -1 \quad \text{in } \Omega \quad (20)$$

$$\nabla^2 U_2 - M \frac{\partial U_2}{\partial x} = -1 \quad \text{in } \Omega \quad (21)$$

with the boundary conditions

$$U_1 = U_2 = 0 \quad \text{on } \partial\Omega \quad (22)$$

One can solve the equation 20 with homogeneous boundary conditions (22) for U_1 . For simplicity use U in the place of U_1 . Applying RBF-FD method to equation 20 gives,

$$\sum_{j=1}^{n_i} C_{ij} U_{ij} + M \sum_{j=1}^{n_i} D_{ij} U_{ij} = -1 \quad (23)$$

where, n_i is the number of neighbourhood points, C_{ij} is the weights corresponding to ∇^2 , D_{ij} are the weights corresponding to $\frac{\partial}{\partial x}$ for each nodal point x_i , $i = 1, 2, \dots, n$. It is obvious that the Dirichlet boundary conditions can be substituted in equation (23) and this leads to the following system of equations.

$$AU = b \quad (24)$$

where, U is an unknown vector which consists of U values at all interior points, b is a known vector and A is a coefficient matrix. When the system is solved for $U_1(M)$ then $U_2(M) = U_1(-M)$ and $V(x, y)$, $B(x, y)$ can be calculated by using 12. The system of equations (18) and (19) can be solved directly, in that case, co-efficient matrix is of order $2n \times 2n$.

4. Numerical results

The MHD flow through a pipe of infinite length with rectangular cross-section has been considered. Conducting fluid flows along the z -axis. Since the cross-sectional analysis is one of the powerful approaches to visualize three-dimensional flows, the flow solution is visualized along the rectangular duct. The dimensions of rectangular duct cross-section are $0 \leq x \leq 1$, $-1 \leq y \leq 1$. A constant magnetic field B_0 is acting in the XY plane and forming an angle with the y -axis. The solutions are presented for different grid sizes and different Hartmann numbers ranging from 1 to 1000 for the case that the magnetic field parallel to the x -axis. For, $\alpha = \frac{\pi}{2}$ the solutions are compared with the analytical solution stated in [38] and classical Finite Difference method. Also, the contour plots are presented for $\alpha = \frac{\pi}{3}$ and $\alpha = \frac{\pi}{4}$. Validation of RBF-FD Scheme is performed by comparing the contours for different grid sizes and different Hartmann numbers with equally spaced points.

Errors have been calculated using supremum norm and the rate of convergence is calculated using the formula

$$rate = \frac{\log E_h - \log E_{h/2}}{\log 2} \quad (25)$$

where, E_h and $E_{h/2}$ are the errors obtained with grid sizes h and $h/2$ respectively. Table [2], [3], [4] and [5] show that the error obtained from RBF methods is less when compared to the Finite Difference method. In this paper, the error analysis has been done using MQ. The errors and rate of convergence have been computed for velocity and the induced magnetic field with FDM, RBF-FD (MQ) method is presented in Table [6] and [7]. Accuracy of the RBF-FD method can be improved by varying the shape parameter in MQ. From Table [6,7] it is clear that the error is minimized as M increases and h decreases. As the Hartmann number increases RBF-FD gives better solution than Finite Difference method. The behaviour of velocity and magnetic field are visualized as a surface plot in figure [1] and [2]. For $\alpha = \pi/3$ and $\pi/4$ the velocity and induced magnetic field contours (using RBF-FD method) are given in Figure [4]. The results obtained from RBF-FD method and FD method are compared with the exact solution as seen in contours presented in figure [3]. For different grid sizes, the error obtained from RBF-FD are presented in figure [5]. For the fixed grid size $1/40$ and $1/80$, the error for different Hartmann numbers has been presented in Fig [6,7]. It is observed that as Hartmann number increases, the numerical solutions from RBF-FD method become closer to the analytical solution when compared with Finite Difference Method.

Table 2. Local truncation error of velocity profile for RBF-FD method.

h	M=1	M=10	M=50	M=100	M=200
1./10	3.03E-04	9.13E-04	2.30E-03	0.0026	0.0029
1./20	8.30E-05	2.17E-04	8.71E-04	0.0013	0.0021
1./25	5.30E-05	1.39E-04	5.98E-04	6.97E-04	0.0010
1./40	2.10E-05	3.50E-05	2.78E-04	4.42E-04	6.65E-04
1./50	2.70E-05	1.72E-05	1.84E-04	5.14E-04	5.58E-04
1./80	3.14E-06	7.10E-06	5.83E-05	3.00E-04	3.25E-04

Table 3. Local truncation error of induced magnetic field for RBF-FD method.

h	M=1	M=10	M=50	M=100	M=200
1./10	1.10E-05	2.40E-04	9.20E-04	0.0019	0.0029
1./20	4.00E-06	2.20E-04	8.20E-04	0.0013	0.0021
1./25	2.00E-06	1.45E-04	6.27E-04	9.44E-04	0.001
1./40	1.00E-06	3.60E-05	2.87E-04	4.22E-04	6.65E-04
1./50	1.00E-06	2.70E-05	1.88E-04	3.19E-04	4.88E-04
1./80	2.32E-07	9.00E-06	5.38E-05	9.01E-05	2.25E-04

Table 4. Local truncation error of velocity profile for Finite Difference method.

h	M=1	M=10	M=50	M=100	M=200
1./10	3.27E-04	0.0016	4.30E-03	0.0037	0.0036
1./20	8.40E-05	3.76E-04	0.0019	0.0022	0.0017
1./25	5.40E-05	2.34E-04	0.0015	0.0018	0.0015
1./40	2.20E-05	9.20E-05	5.56E-04	9.09E-04	0.0011
1./50	1.40E-05	5.90E-05	3.34E-04	6.40E-04	0.001
1./80	8.26E-06	1.00E-05	1.27E-04	5.63E-04	6.13E-04

Table 5. Local truncation error of induced magnetic field for Finite Difference method.

h	M=1	M=10	M=50	M=100	M=200
1./10	1.30E-05	0.0016	4.30E-03	0.0035	0.0039
1./20	4.00E-06	3.75E-04	0.0019	0.0022	0.0017
1./25	2.00E-06	2.33E-04	0.0015	0.0018	0.0015
1./40	1.00E-06	9.20E-05	5.56E-04	9.09E-04	0.0011
1./50	1.00E-06	5.90E-05	3.34E-04	6.40E-04	0.001
1./80	7.14E-07	2.00E-05	1.27E-04	3.15E-04	6.13E-04

Table 6. Error Analysis for Velocity Profile.

M	h	Velocity rate			
		FD	RBF-FD	FD	RBF-FD
1	1/10	3.27E-04	3.03E-04	-	-
1	1/20	8.40E-05	8.30E-05	1.960829	1.868135
1	1/40	2.20E-05	2.10E-05	1.932886	1.982722
1	1/80	8.26E-06	3.14E-06	1.41329	2.641553
10	1/10	1.60E-03	9.13E-04	-	-
10	1/20	3.76E-04	2.17E-04	2.089267	2.07292
10	1/40	9.20E-05	3.50E-05	2.031027	2.301454
10	1/80	2.00E-05	7.10E-06	2.201634	2.301464
50	1/10	4.40E-03	2.80E-04	-	-
50	1/20	1.90E-03	8.71E-04	1.211504	1.684682
50	1/40	5.56E-04	2.79E-04	1.772843	1.642408
50	1/80	1.62E-04	5.83E-05	1.779091	2.258697
100	1/10	3.70E-03	2.10E-03	-	-
100	1/20	2.20E-03	1.20E-03	0.750022	0.807355
100	1/40	9.09E-04	4.42E-04	1.275151	1.440916
100	1/80	5.63E-04	1.01E-04	0.691145	2.129691
200	1/10	3.60E-03	1.70E-03	-	-
200	1/20	1.70E-03	1.20E-03	1.082462	0.5025
200	1/40	1.10E-03	6.65E-04	0.628031	0.851608
200	1/80	8.13E-04	2.25E-04	0.436176	1.563429
400	1/80	7.06E-04	1.32E-05	-	-
500	1/40	7.24E-04	5.59E-04	-	-
1000	1/40	5.29E-04	3.68E-04	-	-

Table 7. Error Analysis for induced Magnetic Field.

M	h	Magnetic Field rate			
		FD	RBF-FD	FD	RBF-FD
1	1/10	3.27E-04	3.03E-04	-	-
1	1/20	8.40E-05	8.30E-05	1.960829	1.868135
1	1/40	2.20E-05	2.10E-05	1.932886	1.982722
1	1/80	8.26E-06	3.14E-06	1.41329	2.641553
10	1/10	1.60E-03	9.13E-04	-	-
10	1/20	3.76E-04	2.17E-04	2.089267	2.07292
10	1/40	9.20E-05	3.50E-05	2.031027	2.301454
10	1/80	2.00E-05	7.10E-06	2.201634	2.301464
50	1/10	4.40E-03	2.80E-04	-	-
50	1/20	1.90E-03	8.71E-04	1.211504	1.684682
50	1/40	5.56E-04	2.79E-04	1.772843	1.642408
50	1/80	1.62E-04	5.83E-05	1.779091	2.258697
100	1/10	3.70E-03	1.95E-03	-	-
100	1/20	2.20E-03	1.10E-03	0.750022	0.825971
100	1/40	9.09E-04	4.22E-04	1.275151	1.382189
100	1/80	3.15E-04	9.01E-05	1.528928	2.227644
200	1/10	1.90E-03	1.20E-03	-	-
200	1/20	1.70E-03	1.00E-03	0.160465	0.263034
200	1/40	7.10E-04	6.50E-04	1.259644	0.621488
200	1/80	4.13E-04	1.01E-04	0.781677	2.686084
400	1/80	7.06E-04	1.30E-04	-	-
500	1/40	7.24E-04	5.52E-04	-	-
1000	1/40	5.24E-04	3.64E-04	-	-

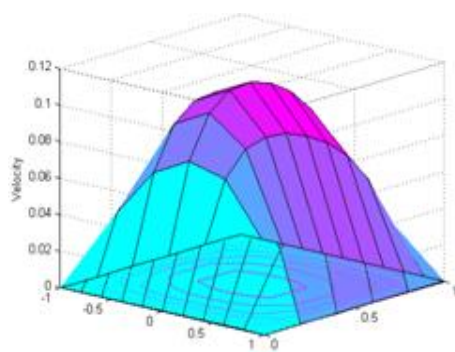
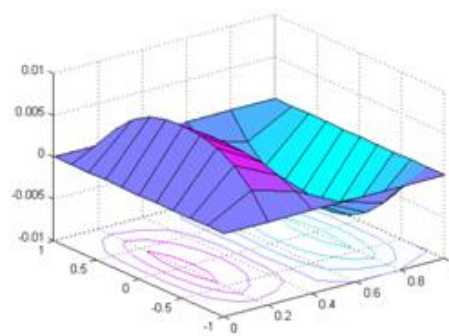
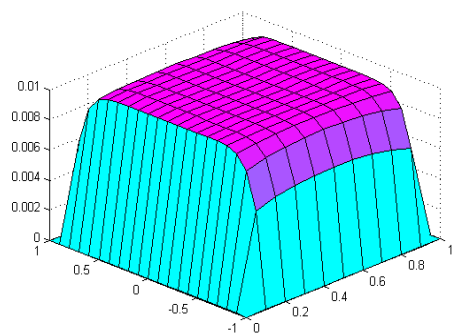
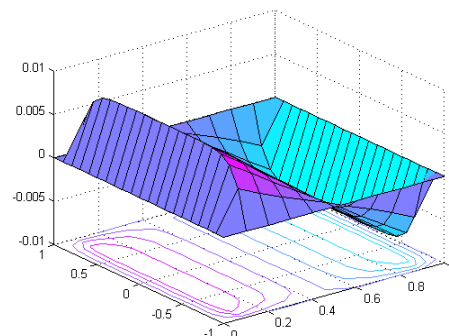
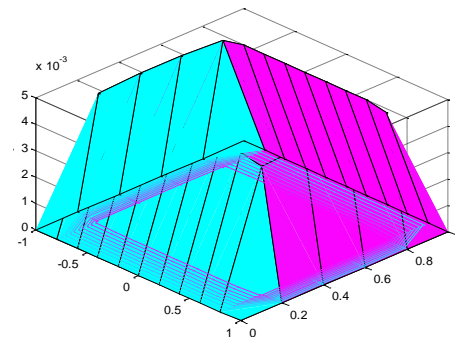
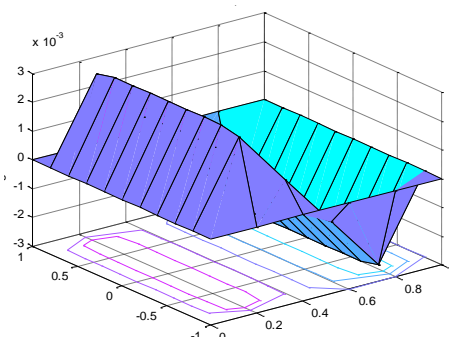
(a) $M=1$ (b) $M=1$ (c) $M=50$ (d) $M=50$ (e) $M=100$ (f) $M=100$

Fig. 1. Surface plot with contour lines of Velocity and Magnetic Field for $M=1,50,100$.

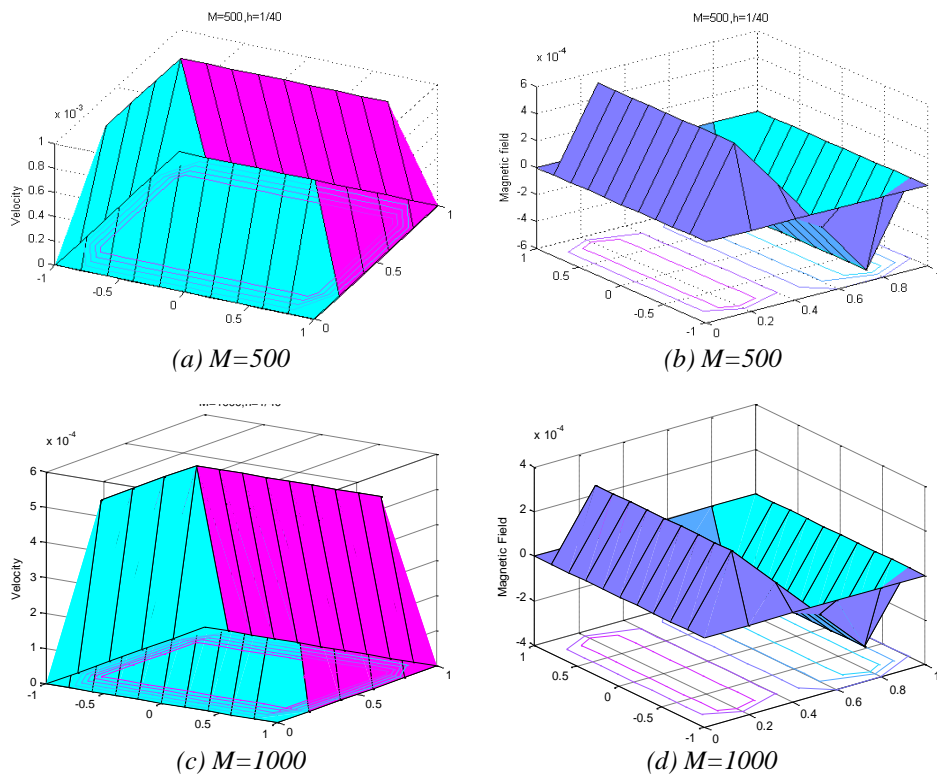
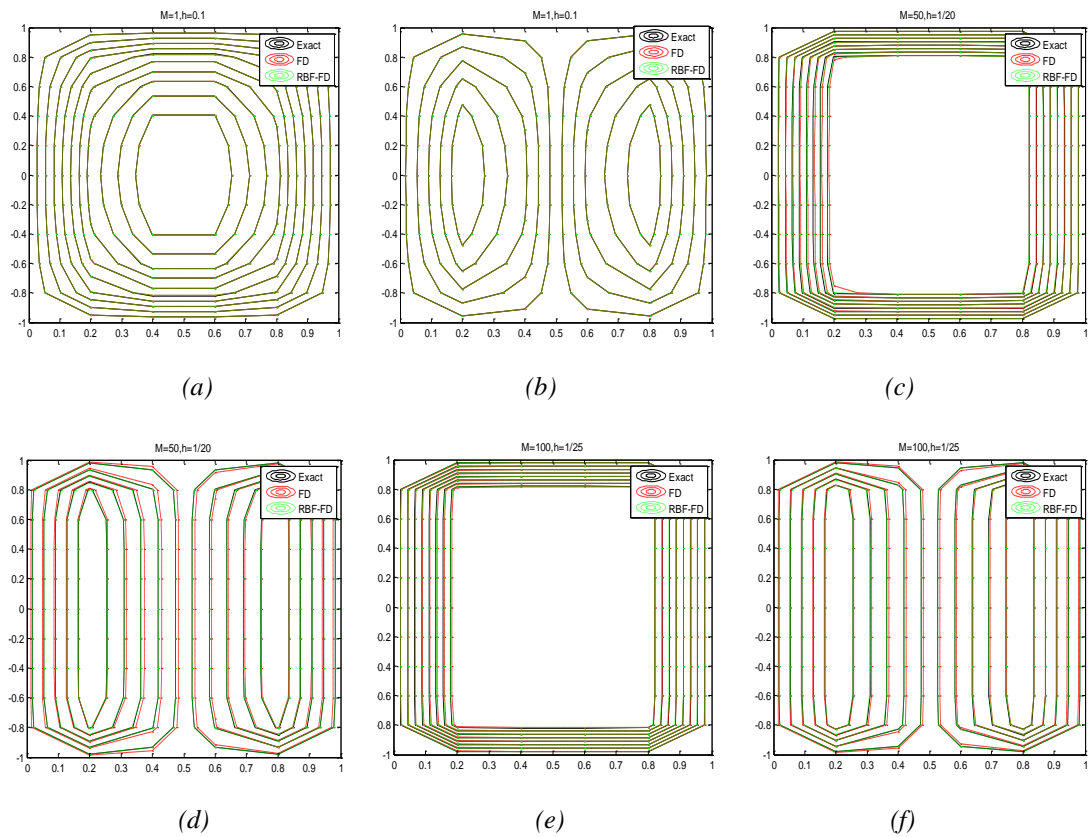


Fig. 2. Surface plots with contour lines of Velocity and Magnetic field for $M=500$ and $M=1000$.



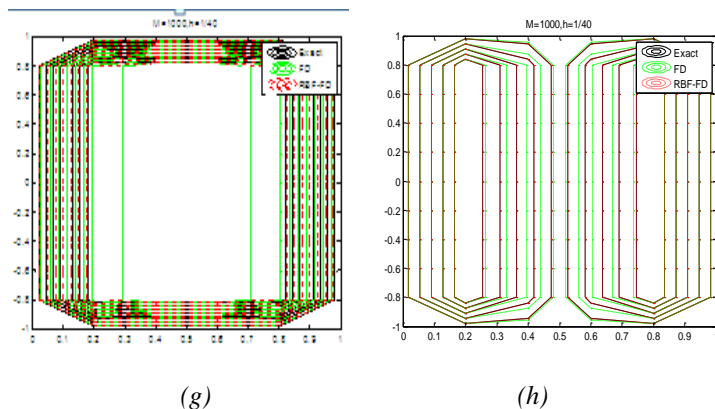


Fig. 3. Velocity and Magnetic field profile for Hartmann numbers $M=1, 50, 100, 1000$.

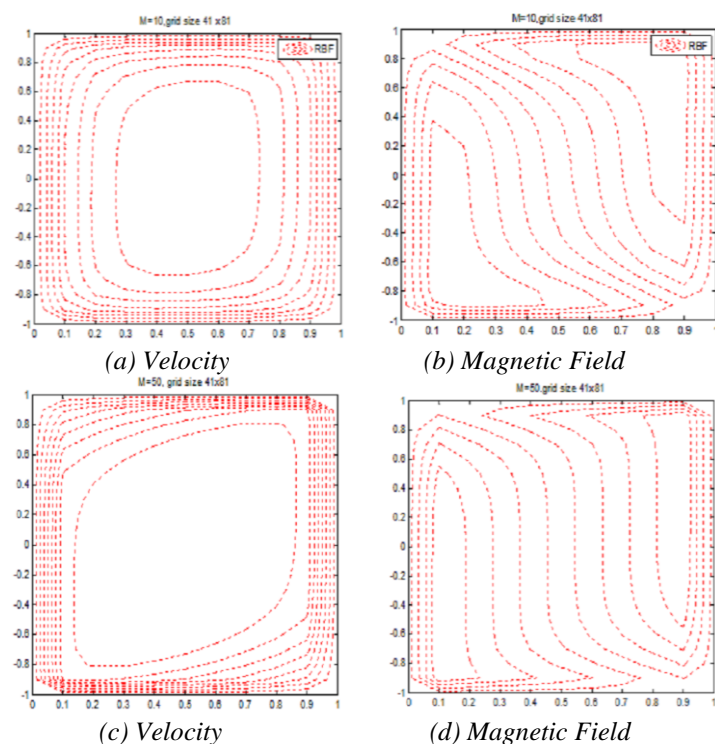


Fig. 4. (a), (b) velocity and magnetic field for Hartmann number $M = 10$, grid size 41×81 & $\alpha = \pi/4$, and (c), (d) velocity and magnetic field for Hartmann number $M = 50$, grid size 41×81 and $\alpha = \pi/3$.

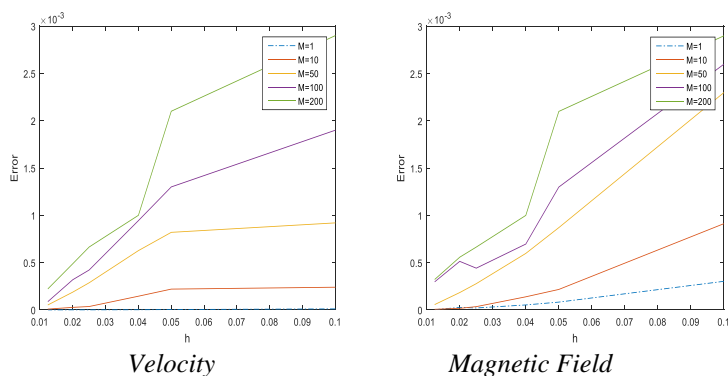


Fig. 5. Error obtained from RBF-FD method for the grid sizes $h=1/10, 1/20, 1/25, 1/40, 1/50, 1/80$.

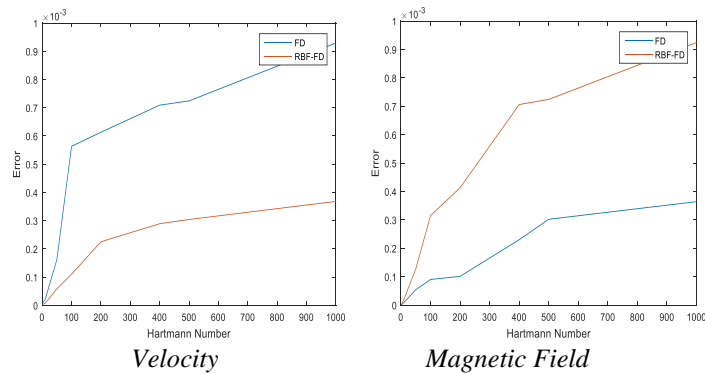


Fig. 6. Comparison of Error from FD method and RBF-FD method for Hartmann numbers $M=1, 10, 50, 100, 200, 400, 500, 1000$ when $h=1/80$.

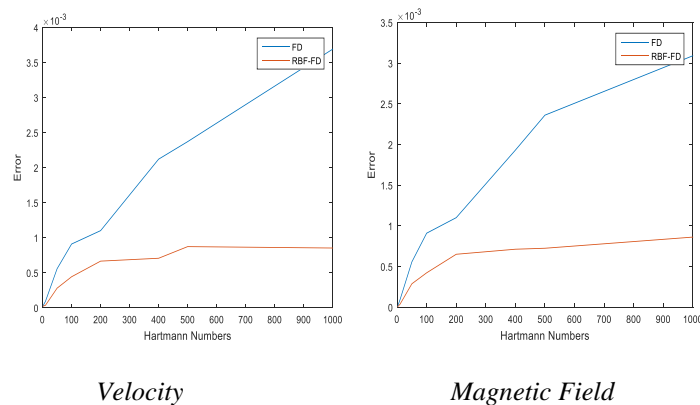


Fig. 7. Comparison of Error from FD method and RBF-FD method for Hartmann numbers $M=1, 10, 50, 100, 200, 400, 500, 1000$ when $h=1/40$.

5. Conclusion

In this present article, the numerical solution of MHD duct flow coupled equation under an external oblique field. This solution has been computed using the classical Finite Difference method and RBF-FD method. The solutions can be obtained for the wide range of Hartmann numbers ($1 < M < 1000$) which could not be done in many of the existing methods (computationally RBF-FD method is not expensive). As the Hartmann number increases the flow becomes laminar in the centre of the duct. Even though the scattered distribution of grids is possible in RBF-FD, uniform grid sizes have been taken to compare the results with standard FDM. It is observed that for higher Hartmann numbers, the error of proposed RBF-FD is less than that of FDM. In our future work, the same method can be applied to partially conduct walls, conducting wall of a cross-section of the shape circle, triangle, hexagon and annulus.

References

- [1] J. Hartmann, F. Lazarus, *Mat Fys Med* **15**, 1 (1937).
- [2] J. A. Shercliff, *In Proc Camb Phil Soc, Cambridge Univ* **49**, 136 (1953).
- [3] C. C. Chang, T. S. Lundgren, *Angew Math Phy* **12**.
- [4] R. R. Gold, *J. Fluid Mech*, **13**, 505 (1962).
- [5] M. Tezer-Sezgin, *Computer Fluids* **33**, 533 (2004).
- [6] J. L. B. Singh, *Ind. J. Pure Appl Math.* **9**, 101 (1978).
- [7] J. L. B. Singh, *Ind. J. Tech.* **17**, 184 (1979).

- [8] M. Tezer-Sezgin, *J. Numer Methods Fluids* **18**, 937 (1994).
- [9] H.-W. Liu, S.-P. Zhu et al., *Aziam J.* **44**, 305 (2002).
- [10] M. Chutial, P. N. Deka, *Int. J. Energy Technol.* **6**, 1 (2014).
- [11] J. L. B. Singh, *J. Numer Methods Eng.* **18**, 1104 (1982).
- [12] B. Singh, J. Lal, *Int. J. Numer Method Fluids*, 291 (1984).
- [13] M. Tezer-Sezgin, S. Köksal, *Int. J. Numer Method Eng* **28**, 445 (1989).
- [14] Z. Demendy, T. Nagyc, *Acta Mechanica* **123**, 135 (1997).
- [15] A. I.Nesliturk, M. Tezer-Sezgin, *Comp Methods Appl. Mech. Eng.* **194**, 1201 (2005).
- [16] D. M. Hossein Hosseinzadeh, Mehdi Dehghan, *Appl. Math. Model* **37**, 2337 (2013).
- [17] R. L. Hardy, *J. Graphical Re.s* **76**, 1905 (1971).
- [18] R. Hardy, *Computer Math. Appl.* **19**, 163 (1990).
- [19] E. Kansa, *Computer Math. Appl.* **19**, 127 (1990).
- [20] E. Kansa, *Computer Math. Appl.* **19**, 147 (1990).
- [21] G. B. Wright., B. Fornberg, *J. Computational Phy.* **212**, 99 (2006).
- [22] R. Franke, *Math. Comp.* **38**, 181 (1982).
- [23] Y. Sanyasiraju, G. Chandhini, *Int. J. Numer Method Eng.* **72**, 352 (2007).
- [24] Y. Sanyasiraju, G. Chandhini, *J. Computational Phy.* **227**, 8922 (2008).
- [25] M. M. Victor Bayona, M. Kindelan, *J. Computational Phy.* **230**, 7384 (2011).
- [26] M. M. Victor Bayona, M. Kindelan, *J. Comput. Phys.* **231**, 2466 (2012).
- [27] G. B. W. M. K. L. F. Varun Shankar, *J. Scientific Comput.* **63**, 745 (2015).
- [28] E. B. Fornberg, *J. Computational Phy.* **230**, 2270 (2011).
- [29] B. Fornberg, N. Flyer, *Siam* **87**, 201 (2015).
- [30] G. A. Natasha Flyer, *J. Computaional Phy.* **316**, 39 (2016).
- [31] B. F. Bradley Martin, *Eng. Anal. Boundary Elements* **79**, 38 (2017).
- [32] M. Prasanna Jeyanthi, *Int. Conference Math. Sci.*, 380 (2014).
- [33] G. S. Dulikravich, S. R. Lynni, *Int. J. Non-Linear Mechanics* **32**, 923 (1997).
- [34] G. S. D. M. J. Colaço, *J. Phy. Chem. Solids* **67**, 1965 (2006).
- [35] M. J. Colaço, G. S. Dulikravich, *Int. J. Heat Mass Trans.* **52**, 5932 (2008).
- [36] E. L. B. Fornberg, G. Wright, *Comput. Math. Appl.* **47**, 37 (2004).
- [37] B. F. Bradley Martin, A. St-Cyr, *Geophysics* **80**, 137 (2015).
- [38] J. A. Shercliff, *American J. Phy.* **34**, 1204 (1966).